ACS NANO

www.acsnano.org

PERSPECTIVE

Phononics of Graphene and Related Materials

Alexander A. Balandin

Cite This: *ACS Nano* 2020, 14, 5170–5178

Read Online

ACCESS | Metrics & More | Article Recommendations

ABSTRACT: In this Perspective, I present a concise account concerning the emergence of the research field investigating the phononic and thermal properties of graphene and related materials, covering the refinement of our understanding of phonon transport in two-dimensional material systems. The initial interest in graphene originated from its unique linear energy dispersion for electrons, revealed in exceptionally high electron mobility, and other exotic electronic and optical properties. Electrons are not the only elemental excitations influenced by a reduction in dimensionality. Phonons—quanta of crystal lattice vibrations—also demonstrate an extreme sensitivity to the number of atomic planes in the few-layer graphene, resulting in unusual heat conduction properties. I outline recent theoretical and experimental developments in the field and discuss how the prospects for the mainstream electronic application of graphene, enabled by its high electron mobility, gradually gave way to emerging real-life products based on few-layer graphene, which utilize its unique heat conduction rather than its electrical conduction properties.

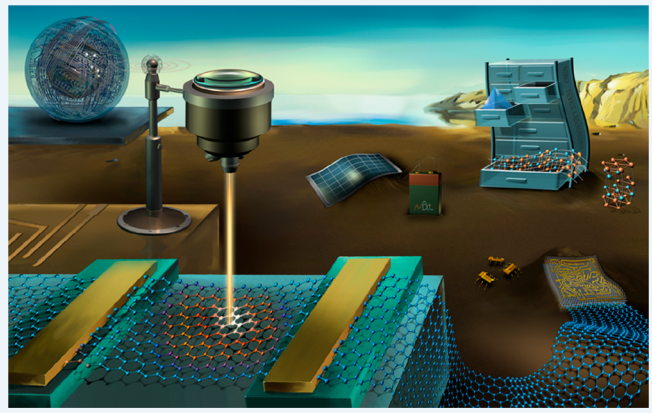

The field of *phononics*[1] comprises the study of quanta of crystal lattice vibrations, whose characteristics influence elastic, acoustic, and thermal properties of bulk and nanostructured materials.[1−3] Phononics of lower-dimensional material systems is particularly interesting, enabling one to elucidate the physics of crystal lattice vibrations and to engineer the phonon spectrum to achieve new functionalities of the materials. Graphene—a monatomic plane of sp^2-hybridized carbon atoms—is an excellent example of a material system of low dimensionality. The initial interest in graphene originated from its unique *linear* energy dispersion for electrons, revealed in an unusually high charge carrier mobility, and other exotic electronic and optical properties.[4−8] Electrons are not the only elemental excitations influenced by a reduction in dimensionality that behave significantly differently from their counterparts in three-dimensional (3D) bulk crystals. Phonons—both optical and acoustic—also demonstrate significant sensitivity to the number of atomic planes as the sample thickness approaches the single-atomic-plane limit. It is no coincidence that monitoring the Raman spectral signatures of graphene's optical phonons—G peak and 2D band—became a standard technique for the identification of graphene and for counting the number of atomic planes in few-layer graphene (FLG).[9−11] The adoption of Raman spectroscopy of graphene for this purpose became instrumental in the proliferation of graphene research: It is much easier to take a Raman spectrum than to conduct low-temperature transport measurements to identify single-layer graphene, as was done previously.

> Apart from the intriguing fundamental science, the discovery of unique phonon transport characteristics of graphene has motivated numerous studies of practical use of graphene and few-layer graphene in thermal composites and coatings.

Acoustic phonons, which are the dominant heat carriers in many materials, demonstrate a similar sensitivity to the number of atomic planes in FLG, changing their ability to conduct heat.[12−14] Graphene is not exactly a *true* two-dimensional (2D) system for phonons, owing to the out-of-plane atomic motion, but it is as close as one can get to a 2D system for phonons in the

Published: April 27, 2020

Downloaded via UNIV OF CALIFORNIA RIVERSIDE on June 5, 2020 at 00:16:43 (UTC).
See https://pubs.acs.org/sharingguidelines for options on how to legitimately share published articles.

ACS Publications

© 2020 American Chemical Society

https://dx.doi.org/10.1021/acsnano.0c02718
ACS Nano 2020, 14, 5170–5178

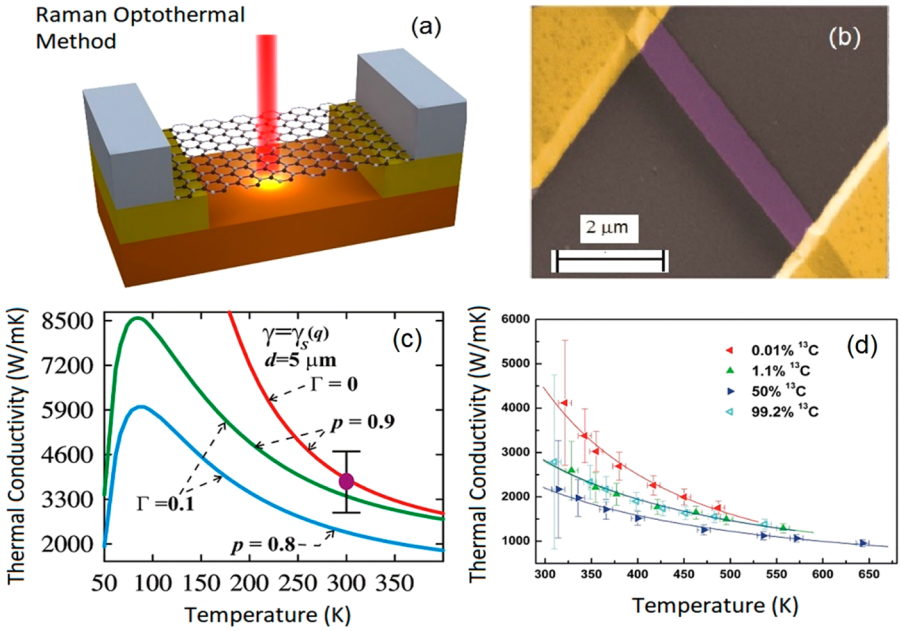

Figure 1. (a) Schematic of micro-Raman optothermal measurements. (b) Scanning electron microscopy image of a graphene ribbon suspended across a trench in a Si/SiO_2 wafer. (c) Calculated thermal conductivity of graphene as a function of temperature for a graphene ribbon with the width of 5 μm. The results are shown for two values of the specularity parameter p and point-defect scattering strength Γ. An experimental data point is provided for comparison. (d) Measured thermal conductivity of suspended CVD graphene with different concentration of ^{13}C isotope. Reprinted with permission from refs 12, 14, and 32. Copyrights 2008 American Chemical Society and 2011 and 2012 Nature Publishing Group, respectively.

physical world.[13−15] The absence of interatomic-plane coupling in graphene and a modified phonon density of states leads to exotic thermal conductivity characteristics such as exceptionally high values and the dependence of the *intrinsic* thermal conductivity on the lateral size of the samples.[14] The availability of FLG has enabled the study of the evolution of thermal conductivity in thin films, which is limited by the intrinsic phonon dynamics rather than by the *extrinsic* effects, such as phonon scattering on rough interfaces.[13] In addition, FLG has made it possible to engineer phonon dispersion in the entire Brillouin zone (BZ) and in the energy range from acoustic to optical phonons by a simple twist of one atomic plane about its surface normal vector with respect to another.[16−20] Apart from the intriguing fundamental science, the discovery of unique phonon transport characteristics of graphene has motivated numerous studies of practical use of graphene and FLG in thermal composites and coatings.[21−26]

THERMAL CONDUCTIVITY OF GRAPHENE AND FEW-LAYER GRAPHENE

The first experimental measurements of thermal conductivity of graphene were performed using a noncontact Raman optothermal method.[12−15] The Raman G peak of graphene is narrow, and its position is sensitive to temperature.[27,28] These attributes of the G peak enable researchers to use the peak's calibrated spectral position to determine a local temperature of the sample. The atomic thickness of graphene, which limits the heat flux, provides an opportunity to use a Raman spectrometer with a conventional low-power laser to measure the highly conductive crystalline materials. The suspension of the graphene sample is another essential consideration of this method and is necessary to determine the power dissipated in the graphene and to ensure the heat flux propagation along a graphene layer toward heat sinks (see Figure 1).[12−15,29−32] Since its introduction, the Raman optothermal technique has been extended to a range of other 2D materials beyond graphene.[33]

The values of thermal conductivity of high-quality exfoliated *suspended* graphene measured by different groups using the Raman optothermal methods range from ~2000 to ~5000 W/mK near room temperature (RT).[14,15,29−32] The average measured thermal conductivity for high-quality exfoliated graphene is ~3000−4000 W/mK, whereas that of high-quality chemical vapor deposition (CVD) polycrystalline graphene is ~2500 W/mK. The electrical measurements of thermal conductivity of CVD graphene, for example, by the thermal bridge method, revealed ~2500 W/mK near RT.[34,35] The thermal conductivity of graphene supported on a substrate is reduced due to the coupling of graphene phonon modes to the substrate and additional phonon scattering on the graphene−substrate interface.[36] The thermal bridge measurements are considered to be more accurate, but they suffer from experimental uncertainty related to unavoidable sample damage and contamination during the required nanofabrication of the heaters and sensors.[14] Defects in the samples lead to lower thermal conductivity. The range of measured values can be attributed to (i) fundamental size dependence of the thermal conductivity of graphene owing to its 2D nature, (ii) differences in sample quality and geometry, (iii) limited accuracy of all experimental techniques, and (iv) mechanical strain and stress in the suspended samples. One should note that the lower bound of the thermal conductivity of graphene, which exceeds that of basal planes of bulk graphite, is more important than the upper bound. The experimental thermal conductivity of carbon nanotubes has been reported in a similar range of values from ~1760 to 5800 W/mK.[37] The average conductivities for carbon nanotubes are 3000−3500 W/mK.[38,39] The theoretical reports for graphene give a larger range of the thermal conductivity: from ~1000 to 10000 W/mK.[15] However, the theoretical and

https://dx.doi.org/10.1021/acsnano.0c02718
ACS Nano 2020, 14, 5170−5178

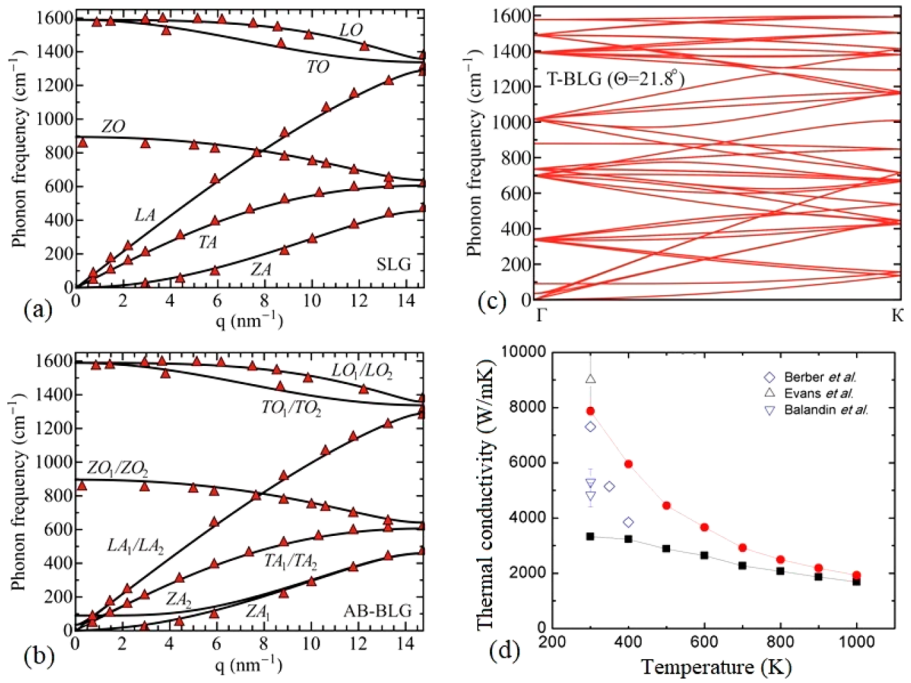

Figure 2. Phonon dispersions in (a) single-layer graphene and (b) AB-stacked bilayer graphene, plotted along the Γ−K direction of the Brillouin zone. (c) Phonon dispersion in twisted bilayer graphene with the twisting angle 21.8°. (d) Thermal conductivity of suspended single-layer graphene as a function of temperature calculated for the phonon number obeying the Bose−Einstein and classical statistics. The data points in (d) shown by diamonds and triangles are from ref 50. Adapted with permission from refs 15, 20, and 50. Copyrights 2017 IOP Publishing, 2015 Royal Society of Chemistry, and 2014 AIP Publishing, respectively.

computational studies are in agreement that the intrinsic thermal conductivity of graphene should be larger than that of carbon nanotubes.[15,40−44]

The thermal conductivity of suspended CVD graphene has been investigated as a function of the density of crystal lattice defects, introduced by the low-energy electron beam irradiation. The near-RT thermal conductivity decreases from ∼2000 to ∼400 W/mK as the defect density increases from 2.0×10^{10} to 1.8×10^{11} cm^{-2}. The thermal conductivity reveals an intriguing saturation behavior at higher concentration of defects.[45] The optothermal Raman technique has been used to investigate phonon transport in twisted bilayer graphene (TBG).[46] In a wide range of examined temperatures (300−750 K), thermal conductivity in TBG is smaller than both in graphene and in naturally AB-stacked bilayer graphene (BLG). Near RT, the thermal conductivity of TBG is smaller than that of graphene by a factor of 2 and is smaller than that of AB-stacked bilayer graphene by a factor of ∼1.35. The drop in thermal conductivity is explained by the emergence of many hybrid-folded phonons in TBG, resulting in more intensive phonon scattering.[46] The possibility of tuning the thermal conductivity of graphene by *isotope engineering* has also been demonstrated (see Figure 1). In view of recent developments pertinent to the phonon hydrodynamic transport in graphene and FLG, which are discussed in a separate section below, future experimental and theoretical challenges will include verification of the thermal conductivity of bulk graphite, accurate measurement of the thermal conductivity of thick films with thicknesses down to FLG and separation of the sample quality effects from those related to fundamental physics.

PHONONS IN GRAPHENE AND BILAYER GRAPHENE

Investigation of heat conduction in graphene has raised the issue of ambiguity in the definition of intrinsic thermal conductivity for 2D crystal lattices. The thermal conductivity, K, limited by the crystal anharmonicity alone, referred to as *intrinsic*, has a finite value in 3D bulk crystals.[47] However, the intrinsic thermal conductivity reveals a logarithmic divergence in 2D crystals, $K \sim \ln(L)$, with the system size, L. This anomalous behavior, which leads to infinite thermal conductivity in 2D systems, is different from the *ballistic* heat conduction in structures smaller in size than the phonon mean-free path (MFP).[14] The logarithmic divergence is related to the dimensionality and corresponding phonon density of states. Graphene is not a true 2D system because it allows for out-of-plane vibrations of the atoms (*e.g.*, associated with the ZA and ZO phonon branches). As a result, the size dependence in graphene may deviate from being logarithmic, and the finite intrinsic limit can be achieved at some size of the sample. Recent theoretical work suggests that convergence to the intrinsic thermal conductivity requires the sample size to be as large as a millimeter.[43] At such a length scale, in real graphene samples, the extrinsic scattering mechanism (*e.g.*, phonon scattering on defects or grain boundaries) would unavoidably start inhibiting the heat conduction. Thus, the actual upper bound of the intrinsic thermal conductivity of graphene may remain an intellectual curiosity rather than a well-defined, observable quantity. The lower bound value is more relevant. If the lower bound is higher than that of a basal plane of graphite, then one can talk about the specific thermal conductivity of graphene, which demonstrates the unique size dependence related to its 2D nature. In other words, the 2D nature of the phonon density of states in graphene results in exceptionally long phonon MFP for the long-wavelength acoustic phonons and corresponding high thermal conductivity.

https://dx.doi.org/10.1021/acsnano.0c02718
ACS Nano 2020, 14, 5170−5178

A number of theoretical and computational studies support this conclusion. A recent experimental study suggested logarithmic size dependence in graphene samples, differing from the linear dependence associated with the ballistic transport regime.[48]

Graphene reveals four graphene sheet in-plane phonon branches: transverse acoustic (TA), longitudinal acoustic (LA), transverse optical (TO), and longitudinal optical (LO); and two out-of-plane acoustic (ZA) and optical (ZO) branches with the displacements perpendicular to the graphene plane. The in-plane acoustic branches are characterized by the linear energy dispersions over most of the BZ except near the zone edge, whereas the out-of-plane ZA branch demonstrates a quadratic dispersion near the zone center $q = 0$, where q is the phonon wavenumber. The number of phonon branches in bilayer graphene is doubled: six additional branches possess nonzero frequency at $q = 0$ and at low frequencies; they are affected by interlayer interactions. The emergence of many folded hybrid phonon branches in TBG is explained by the change of the unit cell size and a corresponding modification of the reciprocal space geometry. The number of polarization branches and their dispersion in TBG depend strongly on the rotation angle (see Figure 2). Twisted bilayer graphene and FLG present interesting material systems where phonon dispersion can be engineered over the entire BZ and range of energies, from acoustic to optical phonons, by rotating the atomic planes with respect to each other. Theoretical studies suggested that ZA phonons primarily determine the specific heat for $T \leq 200$ K, whereas contributions from both in-plane and out-of-plane acoustic phonons are dominant for 200 K $\leq T \leq$ 500 K. In the high-temperature limit, $T > 1000$ K, the optical and acoustic phonons contribute approximately equally to the specific heat.[19,20] The Debye temperature for graphene and TBG is calculated to be around ~1861−1864 K. One can envision the possibility of engineering the thermodynamic properties of materials such as bilayer graphene at the atomic scale by controlled rotation of the sp^2-carbon planes.

Another persistent question in the physics of phonons in graphene is the relative contribution of ZA, LA, and TA phonons to the thermal conductivity. The original models neglected or underestimated ZA phonon contributions in consideration of their low phonon group velocity and large anharmonicity, characterized by the large Grüneisen parameter. Later, it was suggested theoretically that, due to phonon scattering selection rules, ZA phonons are long-lived and can account for a significant portion of overall heat conduction, at least in certain temperature ranges.[40,41,49] However, it was soon noted that graphene's bending, interactions with substrate, and defects can effectively relax this selection rule.[50−52] The most recent development in this field was the exact solution to the linearized phonon Boltzmann transport equation, which includes three-phonon and *four-phonon* scattering processes.[53] It turned out that the reflection symmetry in graphene, which forbids three-ZA phonon scattering, allows four-ZA processes. As a result, the large phonon population of the low-energy ZA branch originating from the quadratic phonon dispersion leads to the four-phonon scattering rates, which are higher than the three-phonon scattering rates at RT. The relative contribution of the ZA phonon branch is correspondingly reduced to be lower than those of the LA and TA branches.[53] The presently available formalism for the four-phonon processes in graphene uses empirical potentials, known to under-predict the thermal conductivity. In the future, theoretical efforts will likely be focused either on calculating the force constants from first-principles instead of from the empirical potentials or on improving the empirical potentials to recover the experimentally measured values of the thermal conductivity of graphite and then using these values to simulate the thermal properties of graphene.

LANDAU SECOND SOUND AND PHONON HYDRODYNAMICS IN GRAPHENE

Another possible explanation for the exceptionally high thermal conductivity of graphene and FLG originates from the concept of phonon hydrodynamic transport and the closely related phenomenon of the second sound. The second sound in superfluid helium was first described as a collective wave by Landau.[54−56] In this description, the "phonon gas" was treated as a particle gas in which harmonic phonon density oscillations could be propagated. In addition to the regular sound velocity, $u_1 = (\partial p/\partial \rho)^{1/2}$, Landau introduced the second sound velocity of the collective excitations, $u_2 = (Ts^2\rho_s/C\rho_n)^{1/2}$, to describe the propagation of the fluctuations in entropy and temperature (here, p is the pressure, and ρ_s and ρ_n are the mass densities of the "superfluid" and "normal" liquids, respectively, C is the heat capacity, and s is the entropy potential).[54] The idea was general enough to suggest the possibility of such phenomena of collective waves in different solids.[57] Phonons in the hydrodynamic regime can form packets that change the typical diffusive behavior of heat and make it propagate as a wave, with the corresponding phenomenon of the second sound, where a localized heating perturbation generates two sound wave fronts.

> Another possible explanation for the exceptionally high thermal conductivity of graphene and few-layer graphene originates from the concept of phonon hydrodynamic transport and the closely related phenomenon of the second sound.

In conventional bulk materials, the phonon hydrodynamic transport regime only occurs at low temperatures, in a rather narrow range between the ballistic and diffusive phonon transport regimes. Using the perturbation theory terminology, one can state that the phonon hydrodynamic transport reveals itself when the normal phonon−phonon scattering processes, which conserve the phonon momentum, become much more predominant than the three-phonon Umklapp scattering processes, which reverse the reduced momentum direction and create resistance to heat flux. The normal phonon scattering alone cannot dissipate a heat flux and returns the system to the thermal equilibrium. These conditions are only met at low temperature in conventional bulk crystals. It has been suggested theoretically that phonon hydrodynamic conduction can occur in graphene over a wide temperature range, owing to the 2D nature of graphene.[58,59] Accounting for the hydrodynamic collective phonon propagation results in high values of thermal conductivity of graphene, that is, above ~3000 W/mK near RT (see details in ref 59). The recent experimental developments led to the reports of the second sound in graphite[60] at temperatures above 100 K and extremely high thermal conductivity of graphite thin films, attributed to the hydrodynamic phonon transport resulting from the phonon dispersion anisotropy.[61] The reported experimental data for

https://dx.doi.org/10.1021/acsnano.0c02718
ACS Nano 2020, 14, 5170−5178

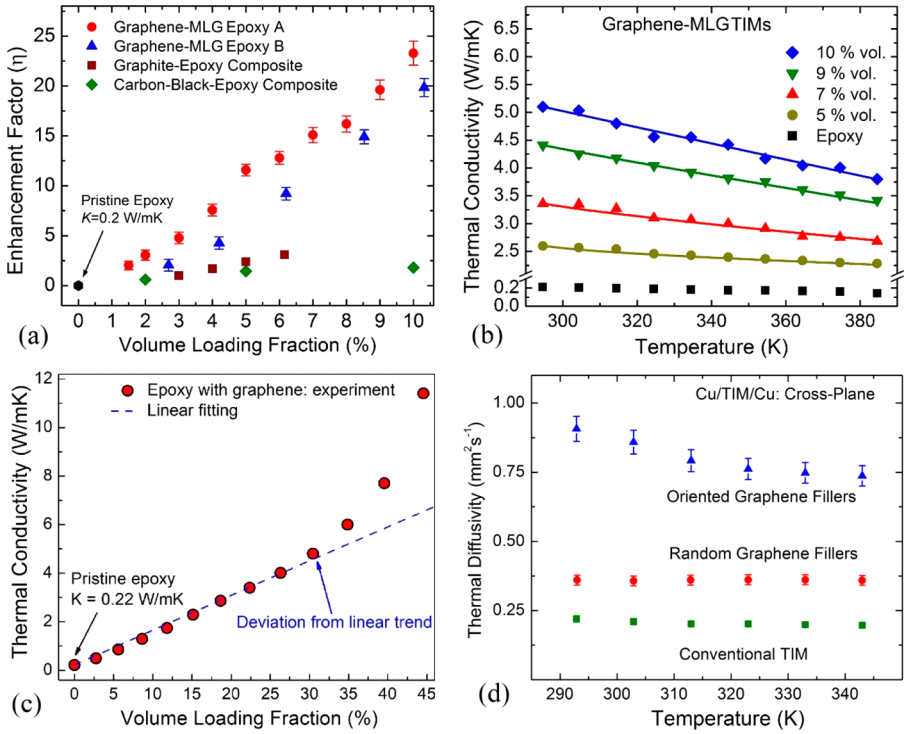

Figure 3. Thermal conductivity of the graphene composites. (a) Thermal conductivity enhancement factor as a function of the filler loading fraction. (b) Temperature-dependent thermal conductivity of graphene−epoxy composites for different graphene loadings. (c) Thermal conductivity of the epoxy composites with graphene at high filler loading. Thermal conductivity depends linearly on the loading until reaching a threshold value, after which it becomes superlinear, indicating the onset of the thermal percolation transport regime. (d) Apparent thermal diffusivity of Cu−TIM−Cu sandwiches with graphene-enhanced thermal interface materials (TIMs) and that of a reference TIM without graphene. Note the importance of graphene filler orientation. Adapted with permission from refs 21, 23, 26, and 62. Copyrights 2012 American Chemical Society, 2012 AIP Publishing, 2018 American Chemical Society, and 2015 Elsevier, respectively.

thin films of graphite show increasing thermal conductivity with decreasing thickness, reaching ~4300 W/mK at RT for 8.5-μm-thick graphite.[61] This value is substantially higher than the conventionally accepted thermal conductivity of bulk graphite.

More experimental studies of the thermal conductivity of graphite thin films over a wider range of thicknesses are needed to make definitive conclusions. One can expect that future theoretical efforts will attempt to reconcile the diffusive or partially diffusive descriptions of thermal transport in graphene and FLG with the hydrodynamic description. There should be a range of parameters, including thicknesses, surface roughness, impurities, isotope content, defects, and temperatures, in which one or the other type of transport dominates. The thickness dependence of the thermal conductivity reported in ref 61 suggests strong phonon boundary scattering effects because strong phonon dispersion modifications are not observed in the examined range of the thicknesses.[61] Determining the roles of specular and diffuse boundary scattering of phonons will be among the future theoretical challenges for graphite thin films and FLG.

THERMAL PROPERTIES OF GRAPHENE-ENHANCED COMPOSITES

Although graphene has the highest intrinsic thermal conductivity, FLG is the most promising material for practical applications in thermal interface materials (TIMs). This assessment is based on the observations that (i) FLG possesses high thermal conductivity, in the range of 500−2000 W/mK, depending on the quality; (ii) FLG has a cross-sectional area larger than that of graphene through which to conduct heat; (iii) the thermal conductivity of FLG degrades less upon exposure to matrix material in the composites; (iv) FLG retains the mechanical flexibility required for thermal coupling to the matrix material; and (v) FLG with variable thickness can be mass produced at low cost. In the context of thermal management, the term "graphene" typically refers to FLG with a thickness range from a few atomic planes to tens of nanometers and lateral dimensions of a few microns. It is imperative that the lateral dimensions be greater than a micrometer (μm) to be above the gray phonon MFP in graphene. In this sense, graphene−FLG fillers used in thermal composites are different from graphite nanoplatelets because they are characterized by smaller lateral dimensions and aspect ratios and from milled graphite fillers with hundreds of nanometers or micrometer thicknesses. Much thicker graphite fillers do not have the flexibility of FLG and, as a result, do not couple well to the matrix. The first studies of graphene composites found that even small loading fractions of graphene fillers can increase the thermal conductivity of composites by up to a factor of 25 (see Figure 3),[21] and these results have been independently confirmed.[24,25] A recent report of composites with high loading of graphene revealed clear signatures of thermal percolation, which enabled the achievement of thermal conductivity of ~12 W/mK, exceeding that of commercial TIMs.[26] Orientation of FLG fillers further increases thermal conductivity of composites.[62,63]

OUTLOOK

As described above, interest in the phononics of graphene and related materials continues to increase, both in fundamental science and in relation to practical applications. Although the

https://dx.doi.org/10.1021/acsnano.0c02718
ACS Nano 2020, 14, 5170−5178

Although graphene has the highest intrinsic thermal conductivity, few-layer graphene is the most promising material for practical applications in thermal interface materials.

initial interest in graphene originated from its unique energy dispersion for electrons, revealed in exotic electronic and optical properties, it is now well understood and conventionally accepted that phonons also demonstrate sensitivity to the number of atomic planes and unusual heat conduction properties originating from the 2D nature of graphene planes. One should expect exciting new developments in the fundamental science of graphene phononics relevant to (i) four-phonon scattering processes and their implications for the phonon selection rules and relative contributions of the LA, TA, and ZA polarization branches; (ii) direct measurements of the acoustic phonon dispersion in graphene and related materials; (iii) further investigation of hydrodynamics phonon transport and the Landau second sounds in graphene, FLG, and graphite thin films; and (iv) detailed study of phonon boundary scattering and interplay of ballistic hydrodynamic and diffusive transport in FLG.

The number of practical applications of graphene related to its phononic properties is growing rapidly. The phononic applications include those that utilize thermal and mechanical properties of the materials, as well as the use of phonon signatures measured by Raman or Brillouin spectroscopy for metrology purposes. A relatively long period of time spent awaiting the "killer" electronic application that would use graphene's exceptionally high electron mobility seems to have been replaced with an explosion of actual applications already on the market that use graphene's non-electronic properties, including thermal, mechanical, surface, and electrochemical properties.[62−80] One should keep in mind here that the term "graphene" in this context includes single-layer graphene and FLG either as layers on a substrate or as a mixture in a composite. A survey of the recent applications of graphene that have already made it to the market shows a wide variety of useful functions that graphene performs, and many of them are related to graphene's phonon transport and heat conduction properties. Specific examples include graphene-enhanced cooling systems for computer processors, epoxy adhesives, coatings, and noncuring TIMs for a wide variety of electronic uses (see Figure 4). All of these developments suggest that it is possible that the true "killer" application, or rather a range of applications, will come from graphene's phononic rather than electronic properties.

It is possible that the true "killer" application, or rather a range of applications, will come from graphene's phononic rather than electronic properties.

AUTHOR INFORMATION

Author

Alexander A. Balandin − *Phonon Optimized Engineered Materials (POEM) Center, Department of Electrical and Computer Engineering, Materials Science and Engineering Program, University of California, Riverside, Riverside, California 92521, United States*

Complete contact information is available at: https://pubs.acs.org/10.1021/acsnano.0c02718

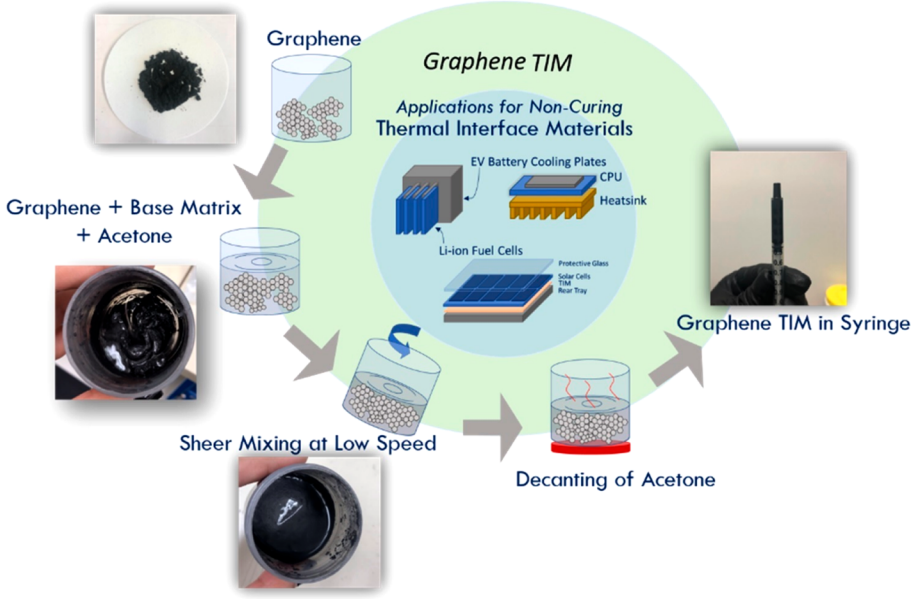

Figure 4. Schematic showing typical practical applications of noncuring thermal interface materials in electronics and the process flow for synthesizing graphene noncuring thermal paste. Graphene is added to the base material with acetone followed by slow-speed sheer mixing. The optimized mixing process separates the graphene and mineral oil mix from the acetone, leaving a smooth graphene paste with proper viscosity that is easy to store and to apply at the interfaces. The synthesis process is scalable and already used by industry. Adapted with permission from ref 72. Copyright 2020 John Wiley & Sons, Inc.

https://dx.doi.org/10.1021/acsnano.0c02718
ACS Nano 2020, 14, 5170−5178

Notes

The author declares no competing financial interest.
This Perspective is based on The Brillouin Medal lecture and publication presented by the author at the PHONONICS 2019: 5th International Conference on Phononic Crystals, Metamaterials, Phonon Transport and Topological Phononics, Tucson, Arizona, USA, 3−7 June 2019.

ACKNOWLEDGMENTS

I thank my former and current Ph.D. students at U.C. Riverside who contributed to graphene phononics research. Special thanks go to Dr. Fariborz Kargar for the recent progress in graphene composite research. I am indebted to the late Professor Evgeni Pokatilov and to Professor Denis Nika for their valuable contributions to the theory of phonon transport in graphene. I would like to acknowledge Sohail Wasif for his help with the table of contents image. My group's phononics research has been supported by NSF, SRC, DARPA, ONR, AFOSR, and DOE.

REFERENCES

(1) Balandin, A.; Nanophononics, A. Phonon Engineering in Nanostructures and Nanodevices. *J. Nanosci. Nanotechnol.* **2005**, *5*, 1015−1022.
(2) Hussein, M. I.; Leamy, M. J.; Ruzzene, M. Dynamics of Phononic Materials and Structures: Historical Origins, Recent Progress, and Future Outlook. *Appl. Mech. Rev.* **2014**, *66*, No. 040802.
(3) El Boudouti, E. H.; Akjouj, A.; Dobrzynski, L.; Djafari-Rouhani, B.; Pennec, Y.; Al-Wahsh, H.; Lévêque, G. One-Dimensional Phononic Crystals. In *Phononics*; Elsevier, 2018; pp 139−270.
(4) Novoselov, K. S.; Geim, A. K.; Morozov, S. v.; Jiang, D.; Zhang, Y.; Dubonos, S. v.; Grigorieva, I. v.; Firsov, A. A. Electric Field Effect in Atomically Thin Carbon Films. *Science* **2004**, *306*, 666−669.
(5) Zhang, Y.; Tan, Y.-W.; Stormer, H. L.; Kim, P. Experimental Observation of the Quantum Hall Effect and Berry's Phase in Graphene. *Nature* **2005**, *438*, 201−204.
(6) Geim, A. K.; Novoselov, K. S. The Rise of Graphene. *Nat. Mater.* **2007**, *6*, 183−191.
(7) Nair, R. R.; Blake, P.; Grigorenko, A. N.; Novoselov, K. S.; Booth, T. J.; Stauber, T.; Peres, N. M. R.; Geim, A. K. Fine Structure Constant Defines Visual Transparency of Graphene. *Science* **2008**, *320*, 1308−1308.
(8) Mak, K. F.; Shan, J.; Heinz, T. F. Seeing Many-Body Effects in Single- and Few-Layer Graphene: Observation of Two-Dimensional Saddle-Point Excitons. *Phys. Rev. Lett.* **2011**, *106*, No. 046401.
(9) Ferrari, A. C.; Meyer, J. C.; Scardaci, V.; Casiraghi, C.; Lazzeri, M.; Mauri, F.; Piscanec, S.; Jiang, D.; Novoselov, K. S.; Roth, S.; Geim, A. K. Raman Spectrum of Graphene and Graphene Layers. *Phys. Rev. Lett.* **2006**, *97*, 187401.
(10) Ferrari, A. C. Raman Spectroscopy of Graphene and Graphite: Disorder, Electron−Phonon Coupling, Doping and Nonadiabatic Effects. *Solid State Commun.* **2007**, *143*, 47−57.
(11) Ferrari, A. C.; Basko, D. M. Raman Spectroscopy as a Versatile Tool for Studying the Properties of Graphene. *Nat. Nanotechnol.* **2013**, *8*, 235−246.
(12) Balandin, A. A.; Ghosh, S.; Bao, W.; Calizo, I.; Teweldebrhan, D.; Miao, F.; Lau, C. N. Superior Thermal Conductivity of Single-Layer Graphene. *Nano Lett.* **2008**, *8*, 902−907.
(13) Ghosh, S.; Bao, W.; Nika, D. L.; Subrina, S.; Pokatilov, E. P.; Lau, C. N.; Balandin, A. A. Dimensional Crossover of Thermal Transport in Few-Layer Graphene. *Nat. Mater.* **2010**, *9*, 555−558.
(14) Balandin, A. A. Thermal Properties of Graphene and Nanostructured Carbon Materials. *Nat. Mater.* **2011**, *10*, 569−581.
(15) Nika, D. L.; Balandin, A. A. Phonons and Thermal Transport in Graphene and Graphene-Based Materials. *Rep. Prog. Phys.* **2017**, *80*, No. 036502.
(16) Gupta, A. K.; Tang, Y.; Crespi, V. H.; Eklund, P. C. Nondispersive Raman D Band Activated by Well-Ordered Interlayer Interactions in Rotationally Stacked Bilayer Graphene. *Phys. Rev. B: Condens. Matter Mater. Phys.* **2010**, *82*, 241406.
(17) Righi, A.; Costa, S. D.; Chacham, H.; Fantini, C.; Venezuela, P.; Magnuson, C.; Colombo, L.; Bacsa, W. S.; Ruoff, R. S.; Pimenta, M. A. Graphene Moiré Patterns Observed by Umklapp Double-Resonance Raman Scattering. *Phys. Rev. B: Condens. Matter Mater. Phys.* **2011**, *84*, 241409.
(18) Cocemasov, A. I.; Nika, D. L.; Balandin, A. A. Phonons in Twisted Bilayer Graphene. *Phys. Rev. B: Condens. Matter Mater. Phys.* **2013**, *88*, No. 035428.
(19) Nika, D. L.; Cocemasov, A. I.; Balandin, A. A. Specific Heat of Twisted Bilayer Graphene: Engineering Phonons by Atomic Plane Rotations. *Appl. Phys. Lett.* **2014**, *105*, No. 031904.
(20) Cocemasov, A. I.; Nika, D. L.; Balandin, A. A. Engineering of the Thermodynamic Properties of Bilayer Graphene by Atomic Plane Rotations: The Role of the Out-of-Plane Phonons. *Nanoscale* **2015**, *7*, 12851−12859.
(21) Shahil, K. M. F.; Balandin, A. A. Graphene-Multilayer Graphene Nanocomposites as Highly Efficient Thermal Interface Materials. *Nano Lett.* **2012**, *12*, 861−867.
(22) Yan, Z.; Liu, G.; Khan, J. M.; Balandin, A. A. Graphene Quilts for Thermal Management of High-Power GaN Transistors. *Nat. Commun.* **2012**, *3*, 827.
(23) Goyal, V.; Balandin, A. A. Thermal Properties of the Hybrid Graphene-Metal Nano-Micro-Composites: Applications in Thermal Interface Materials. *Appl. Phys. Lett.* **2012**, *100*, No. 073113.
(24) Fu, Y. X.; He, Z. X.; Mo, D. C.; Lu, S. S. Thermal Conductivity Enhancement of Epoxy Adhesive Using Graphene Sheets as Additives. *Int. J. Therm. Sci.* **2014**, *86*, 276−283.
(25) Shtein, M.; Nadiv, R.; Buzaglo, M.; Regev, O. Graphene-Based Hybrid Composites for Efficient Thermal Management of Electronic Devices. *ACS Appl. Mater. Interfaces* **2015**, *7*, 23725−23730.
(26) Kargar, F.; Barani, Z.; Salgado, R.; Debnath, B.; Lewis, J. S.; Aytan, E.; Lake, R. K.; Balandin, A. A. Thermal Percolation Threshold and Thermal Properties of Composites with High Loading of Graphene and Boron Nitride Fillers. *ACS Appl. Mater. Interfaces* **2018**, *10*, 37555−37565.
(27) Calizo, I.; Balandin, A. A.; Bao, W.; Miao, F.; Lau, C. N. Temperature Dependence of the Raman Spectra of Graphene and Graphene Multilayers. *Nano Lett.* **2007**, *7*, 2645−2649.
(28) Calizo, I.; Miao, F.; Bao, W.; Lau, C. N.; Balandin, A. A. Variable Temperature Raman Microscopy as a Nanometrology Tool for Graphene Layers and Graphene-Based Devices. *Appl. Phys. Lett.* **2007**, *91*, No. 071913.
(29) Cai, W.; Moore, A. L.; Zhu, Y.; Li, X.; Chen, S.; Shi, L.; Ruoff, R. S. Thermal Transport in Suspended and Supported Monolayer Graphene Grown by Chemical Vapor Deposition. *Nano Lett.* **2010**, *10*, 1645−1651.
(30) Jauregui, L. A.; Yue, Y.; Sidorov, A. N.; Hu, J.; Yu, Q.; Lopez, G.; Jalilian, R.; Benjamin, D. K.; Delkd, D. A.; Wu, W.; Liu, Z.; Wang, X.; Jiang, Z.; Ruan, X.; Bao, J.; Pei, S. S.; Chen, Y. P. Thermal Transport in Graphene Nanostructures: Experiments and Simulations. *ECS Trans.* **2010**, *28*, 73−83.
(31) Chen, S.; Moore, A. L.; Cai, W.; Suk, J. W.; An, J.; Mishra, C.; Amos, C.; Magnuson, C. W.; Kang, J.; Shi, L.; Ruoff, R. S. Raman Measurements of Thermal Transport in Suspended Monolayer Graphene of Variable Sizes in Vacuum and Gaseous Environments. *ACS Nano* **2011**, *5*, 321−328.
(32) Chen, S.; Wu, Q.; Mishra, C.; Kang, J.; Zhang, H.; Cho, K.; Cai, W.; Balandin, A. A.; Ruoff, R. S. Thermal Conductivity of Isotopically Modified Graphene. *Nat. Mater.* **2012**, *11*, 203−207.
(33) Malekpour, H.; Balandin, A. A. Raman-Based Technique for Measuring Thermal Conductivity of Graphene and Related Materials. *J. Raman Spectrosc.* **2018**, *49*, 106−120.
(34) Dorgan, V. E.; Behnam, A.; Conley, H. J.; Bolotin, K. I.; Pop, E. High-Field Electrical and Thermal Transport in Suspended Graphene. *Nano Lett.* **2013**, *13*, 4581−4586.

https://dx.doi.org/10.1021/acsnano.0c02718
ACS Nano 2020, 14, 5170−5178

(35) Yoon, K.; Hwang, G.; Chung, J.; Kim, H. G.; Kwon, O.; Kihm, K. D.; Lee, J. S. Measuring the Thermal Conductivity of Residue-Free Suspended Graphene Bridge Using Null Point Scanning Thermal Microscopy. *Carbon* **2014**, *76*, 77−83.
(36) Seol, J. H.; Jo, I.; Moore, A. L.; Lindsay, L.; Aitken, Z. H.; Pettes, M. T.; Li, X.; Yao, Z.; Huang, R.; Broido, D.; Mingo, N.; Ruoff, R. S.; Shi, L. Two-Dimensional Phonon Transport in Supported Graphene. *Science* **2010**, *328*, 213−216.
(37) Hone, J.; Whitney, M.; Piskoti, C.; Zettl, A. Thermal Conductivity of Single-Walled Carbon Nanotubes. *Phys. Rev. B: Condens. Matter Mater. Phys.* **1999**, *59*, R2514.
(38) Kim, P.; Shi, L.; Majumdar, A.; McEuen, P. L. Thermal Transport Measurements of Individual Multiwalled Nanotubes. *Phys. Rev. Lett.* **2001**, *87*, 215502.
(39) Pop, E.; Mann, D.; Wang, Q.; Goodson, K.; Dai, H. Thermal Conductance of an Individual Single-Wall Carbon Nanotube above Room Temperature. *Nano Lett.* **2006**, *6*, 96−100.
(40) Lindsay, L.; Broido, D. A.; Mingo, N. Flexural Phonons and Thermal Transport in Graphene. *Phys. Rev. B: Condens. Matter Mater. Phys.* **2010**, *82*, 115427.
(41) Lindsay, L.; Broido, D. A. Optimized Tersoff and Brenner Empirical Potential Parameters for Lattice Dynamics and Phonon Thermal Transport in Carbon Nanotubes and Graphene. *Phys. Rev. B: Condens. Matter Mater. Phys.* **2010**, *81*, 205441.
(42) Bonini, N.; Garg, J.; Marzari, N. Acoustic Phonon Lifetimes and Thermal Transport in Free-Standing and Strained Graphene. *Nano Lett.* **2012**, *12*, 2673−2678.
(43) Fugallo, G.; Cepellotti, A.; Paulatto, L.; Lazzeri, M.; Marzari, N.; Mauri, F. Thermal Conductivity of Graphene and Graphite: Collective Excitations and Mean Free Paths. *Nano Lett.* **2014**, *14*, 6109−6114.
(44) Aksamija, Z.; Knezevic, I. Thermal Transport in Graphene Nanoribbons Supported on SiO_2. *Phys. Rev. B: Condens. Matter Mater. Phys.* **2012**, *86*, 165426.
(45) Malekpour, H.; Ramnani, P.; Srinivasan, S.; Balasubramanian, G.; Nika, D. L.; Mulchandani, A.; Lake, R. K.; Balandin, A. A. Thermal Conductivity of Graphene with Defects Induced by Electron Beam Irradiation. *Nanoscale* **2016**, *8*, 14608−14616.
(46) Li, H.; Ying, H.; Chen, X.; Nika, D. L.; Cocemasov, A. I.; Cai, W.; Balandin, A. A.; Chen, S. Thermal Conductivity of Twisted Bilayer Graphene. *Nanoscale* **2014**, *6*, 13402−13408.
(47) Saito, K.; Dhar, A. Heat Conduction in a Three Dimensional Anharmonic Crystal. *Phys. Rev. Lett.* **2010**, *104*, No. 040601.
(48) Xu, X.; Pereira, L. F. C.; Wang, Y.; Wu, J.; Zhang, K.; Zhao, X.; Bae, S.; Tinh Bui, C.; Xie, R.; Thong, J. T. L.; Hong, B. H.; Loh, K. P.; Donadio, D.; Li, B.; Özyilmaz, B. Length-Dependent Thermal Conductivity in Suspended Single-Layer Graphene. *Nat. Commun.* **2014**, *5*, 3689.
(49) Singh, D.; Murthy, J. Y.; Fisher, T. S. Spectral Phonon Conduction and Dominant Scattering Pathways in Graphene. *J. Appl. Phys.* **2011**, *110*, No. 094312.
(50) Wei, Z.; Yang, J.; Bi, K.; Chen, Y. Mode Dependent Lattice Thermal Conductivity of Single Layer Graphene. *J. Appl. Phys.* **2014**, *116*, 153503.
(51) Shen, Y.; Xie, G.; Wei, X.; Zhang, K.; Tang, M.; Zhong, J.; Zhang, G.; Zhang, Y.-W. Size and Boundary Scattering Controlled Contribution of Spectral Phonons to the Thermal Conductivity in Graphene Ribbons. *J. Appl. Phys.* **2014**, *115*, No. 063507.
(52) Feng, T.; Ruan, X.; Ye, Z.; Cao, B. Spectral Phonon Mean Free Path and Thermal Conductivity Accumulation in Defected Graphene: The Effects of Defect Type and Concentration. *Phys. Rev. B: Condens. Matter Mater. Phys.* **2015**, *91*, 224301.
(53) Feng, T.; Ruan, X. Four-Phonon Scattering Reduces Intrinsic Thermal Conductivity of Graphene and the Contributions from Flexural Phonons. *Phys. Rev. B: Condens. Matter Mater. Phys.* **2018**, *97*, No. 045202.
(54) Landau, L. D. Two-Fluid Model of Liquid Helium II. *J. Phys. USSR* **1941**, *5*, 71−90.
(55) Landau, L. D. Theory of the Superfluidity of Helium II. *Phys. Rev.* **1941**, *60*, 356−358.
(56) Landau, L. D. On the Theory of Superfluidity of Helium II. *J. Phys. USSR* **1947**, *11*, 91.
(57) Prohofsky, E. W.; Krumhansl, J. A. Second-Sound Propagation in Dielectric Solids. *Phys. Rev.* **1964**, *133*, A1403−A1410.
(58) Lee, S.; Broido, D.; Esfarjani, K.; Chen, G. Hydrodynamic Phonon Transport in Suspended Graphene. *Nat. Commun.* **2015**, *6*, 6290.
(59) Cepellotti, A.; Fugallo, G.; Paulatto, L.; Lazzeri, M.; Mauri, F.; Marzari, N. Phonon Hydrodynamics in Two-Dimensional Materials. *Nat. Commun.* **2015**, *6*, 6400.
(60) Huberman, S.; Duncan, R. A.; Chen, K.; Song, B.; Chiloyan, V.; Ding, Z.; Maznev, A. A.; Chen, G.; Nelson, K. A. Observation of Second Sound in Graphite at Temperatures Above 100 K. *Science* **2019**, *364*, 375−379.
(61) Machida, Y.; Matsumoto, N.; Isono, T.; Behnia, K. Phonon Hydrodynamics and Ultrahigh−Room-Temperature Thermal Conductivity in Thin Graphite. *Science* **2020**, *367*, 309−312.
(62) Renteria, J.; Legedza, S.; Salgado, R.; Balandin, M. P.; Ramirez, S.; Saadah, M.; Kargar, F.; Balandin, A. A. Magnetically-Functionalized Self-Aligning Graphene Fillers for High-Efficiency Thermal Management Applications. *Mater. Des.* **2015**, *88*, 214−221.
(63) Malekpour, H.; Chang, K. H.; Chen, J. C.; Lu, C. Y.; Nika, D. L.; Novoselov, K. S.; Balandin, A. A. Thermal Conductivity of Graphene Laminate. *Nano Lett.* **2014**, *14*, 5155−5161.
(64) Kholmanov, I.; Kim, J.; Ou, E.; Ruoff, R. S.; Shi, L. Continuous Carbon Nanotube-Ultrathin Graphite Hybrid Foams for Increased Thermal Conductivity and Suppressed Subcooling in Composite Phase Change Materials. *ACS Nano* **2015**, *9*, 11699−11707.
(65) Loeblein, M.; Tsang, S. H.; Pawlik, M.; Phua, E. J. R.; Yong, H.; Zhang, X. W.; Gan, C. L.; Teo, E. H. T. High-Density 3D-Boron Nitride and 3D-Graphene for High-Performance Nano-Thermal Interface Material. *ACS Nano* **2017**, *11*, 2033−2044.
(66) Dai, W.; Lv, L.; Lu, J.; Hou, H.; Yan, Q.; Alam, F. E.; Li, Y.; Zeng, X.; Yu, J.; Wei, Q.; Xu, X.; Wu, J.; Jiang, N.; Du, S.; Sun, R.; Xu, J.; Wong, C. P.; Lin, C.-T. A Paper-Like Inorganic Thermal Interface Material Composed of Hierarchically Structured Graphene/Silicon Carbide Nanorods. *ACS Nano* **2019**, *13*, 1547−1554.
(67) Barani, Z.; Mohammadzadeh, A.; Geremew, A.; Huang, C.; Coleman, D.; Mangolini, L.; Kargar, F.; Balandin, A. A. Thermal Properties of the Binary-Filler Hybrid Composites with Graphene and Copper Nanoparticles. *Adv. Funct. Mater.* **2020**, *30*, 1904008.
(68) Dai, W.; Ma, T.; Yan, Q.; Gao, J.; Tan, X.; Lv, L.; Hou, H.; Wei, Q.; Yu, J.; Wu, J.; Yao, Y.; Du, S.; Sun, R.; Jiang, N.; Wang, Y.; Kong, J.; Wong, C.; Maruyama, S.; Lin, C.-T. Metal-Level Thermally Conductive Yet Soft Graphene Thermal Interface Materials. *ACS Nano* **2019**, *13*, 11561−11571.
(69) Wang, B.; Cunning, B. v.; Kim, N. Y.; Kargar, F.; Park, S.; Li, Z.; Joshi, S. R.; Peng, L.; Modepalli, V.; Chen, X.; Shen, Y.; Seong, W. K.; Kwon, Y.; Jang, J.; Shi, H.; Gao, C.; Kim, G.; Shin, T. J.; Kim, K.; Kim, J.; Balandin, A. A.; Lee, Z.; Ruoff, R. S. Ultrastiff, Strong, and Highly Thermally Conductive Crystalline Graphitic Films with Mixed Stacking Order. *Adv. Mater.* **2019**, *31*, 1903039.
(70) Lewis, J. S; Barani, Z.; Magana, A. S.; Kargar, F.; Balandin, A. A Thermal and Electrical Conductivity Control in Hybrid Composites with Graphene and Boron Nitride Fillers. *Mater. Res. Express* **2019**, *6*, No. 085325.
(71) Fu, Y.; Hansson, J.; Liu, Y.; Chen, S.; Zehri, A.; Samani, M. K.; Wang, N.; Ni, Y.; Zhang, Y.; Zhang, Z.-B.; Wang, Q.; Li, M.; Lu, H.; Sledzinska, M.; Torres, C. M. S.; Volz, S.; Balandin, A. A.; Xu, X.; Liu, J. Graphene Related Materials for Thermal Management. *2D Mater.* **2020**, *7*, No. 012001.
(72) Naghibi, S.; Kargar, F.; Wright, D.; Huang, C. Y. T.; Mohammadzadeh, A.; Barani, Z.; Salgado, R.; Balandin, A. A. Noncuring Graphene Thermal Interface Materials for Advanced Electronics. *Adv. Electron. Mater.* **2020**, *6*, 1901303.
(73) Mahadevan, B. K.; Naghibi, S.; Kargar, F.; Balandin, A. A. Non-Curing Thermal Interface Materials with Graphene Fillers for Thermal Management of Concentrated Photovoltaic Solar Cells. *C* **2020**, *6*, 2.

https://dx.doi.org/10.1021/acsnano.0c02718
ACS Nano 2020, 14, 5170−5178

(74) Jia, J.; Sun, X.; Lin, X.; Shen, X.; Mai, Y. W.; Kim, J. K. Exceptional Electrical Conductivity and Fracture Resistance of 3D Interconnected Graphene Foam/Epoxy Composites. *ACS Nano* **2014**, *8*, 5774−5783.
(75) Pang, Y.; Yang, J.; Curtis, T. E.; Luo, S.; Huang, D.; Feng, Z.; Morales-Ferreiro, J. O.; Sapkota, P.; Lei, F.; Zhang, J.; Zhang, Q.; Lee, E.; Huang, Y.; Guo, R.; Ptasinska, S.; Roeder, R. K.; Luo, T. Exfoliated Graphene Leads to Exceptional Mechanical Properties of Polymer Composite Films. *ACS Nano* **2019**, *13*, 1097−1106.
(76) Kong, L.; Zhang, C.; Wang, J.; Qiao, W.; Ling, L.; Long, D. Free-Standing T-Nb_2O_5/Graphene Composite Papers with Ultrahigh Gravimetric/Volumetric Capacitance for Li-Ion Intercalation Pseudocapacitor. *ACS Nano* **2015**, *9*, 11200−11208.
(77) Xue, S.; Chen, L.; Liu, Z.; Cheng, H. M.; Ren, W. $NiPS_3$ Nanosheet-Graphene Composites as Highly Efficient Electrocatalysts for Oxygen Evolution Reaction. *ACS Nano* **2018**, *12*, 5297−5305.
(78) Berman, D.; Deshmukh, S. A.; Narayanan, B.; Sankaranarayanan, S. K. R. S.; Yan, Z.; Balandin, A. A.; Zinovev, A.; Rosenmann, D.; Sumant, A. V. Metal-Induced Rapid Transformation of Diamond into Single and Multilayer Graphene on Wafer Scale. *Nat. Commun.* **2016**, *7*, 12099.
(79) Ramirez, S.; Chan, K.; Hernandez, R.; Recinos, E.; Hernandez, E.; Salgado, R.; Khitun, A. G.; Garay, J. E.; Balandin, A. A. Thermal and Magnetic Properties of Nanostructured Densified Ferrimagnetic Composites with Graphene - Graphite Fillers. *Mater. Des.* **2017**, *118*, 75−80.
(80) Saadah, M.; Hernandez, E.; Balandin, A. Thermal Management of Concentrated Multi-Junction Solar Cells with Graphene-Enhanced Thermal Interface Materials. *Appl. Sci.* **2017**, *7*, 589.

https://dx.doi.org/10.1021/acsnano.0c02718
ACS Nano 2020, 14, 5170−5178